SuperTIGER Abundances of Galactic Cosmic Rays for the Atomic Number (Z) Interval 30 to 56

Nathan Walsh

ICRC 2021

on behalf of

SuperTIGER Collaboration

N.E. WALSH[1], Y. AKAIKE[2,5], W.R. BINNS[1], R.G. BOSE[1], T.J. BRANDT[2], D.L. BRAUN[1], N. CANNADY[2], W.M. DANIELS[2], P.F. DOWKONTT[1], S.P. FITZSIMMONS[2], D.J. HAHNE[2], T. HAMS[2], M.H. ISRAEL[1], J. KLEMIC[3], J.F. KRIZMANIC[2,5], A.W. LABRADOR[3], R.A. MEWALDT[3], J.W. MITCHELL[2], P. MOORE[1], R.P. MURPHY[1], G.A. DE NOLFO[2], M.A. OLEVITCH[1], B.F. RAUCH[1], K. SAKAI[2,5], F. SAN SEBASTIAN[2], M. SASAKI[2,5], G.E. SIMBURGER[1], E.C. STONE[3], T. TATOLI[2], J.E. WARD[1], M.E. WIEDENBECK[4], W.V. ZOBER[1]

1. Washington University, St. Louis, MO 63130, USA
2. NASA/Goddard Space Flight Center, Greenbelt, MD 20771, USA
3. California Institute of Technology, Pasadena, CA 91125, USA
4. Jet Propulsion Laboratory, California Institute of Technology, Pasadena, CA 91109, USA
5. Center for Research and Exploration in Space Science and Technology (CRESST)

GCR Origin and Acceleration - Volatility Model

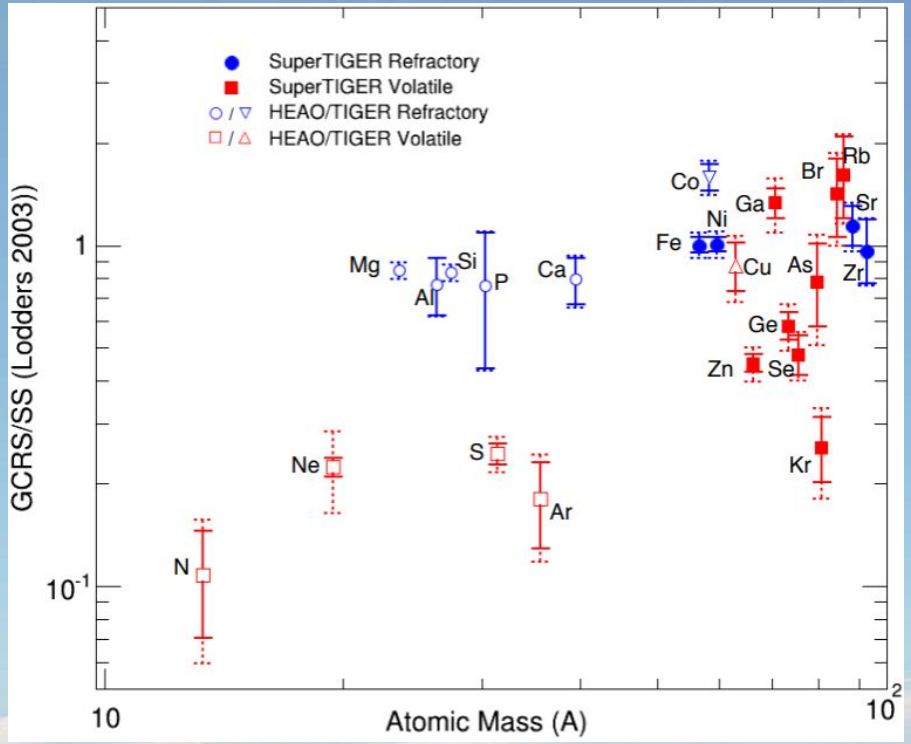

Murphy et al. 2016

- Supernova (SN) shock acceleration is more efficient for particles with high rigidity $R=p/q$
- Refractory elements, with condensation temperatures T_C>~1250K, are more easily embedded in dust grains with high m/q and are therefore preferentially accelerated compared to volatile elements
- Refractory enhancement breaks down for A>60 for GCRS plotted relative to solar system (SS)

GCR Origin and Acceleration - OB Associations

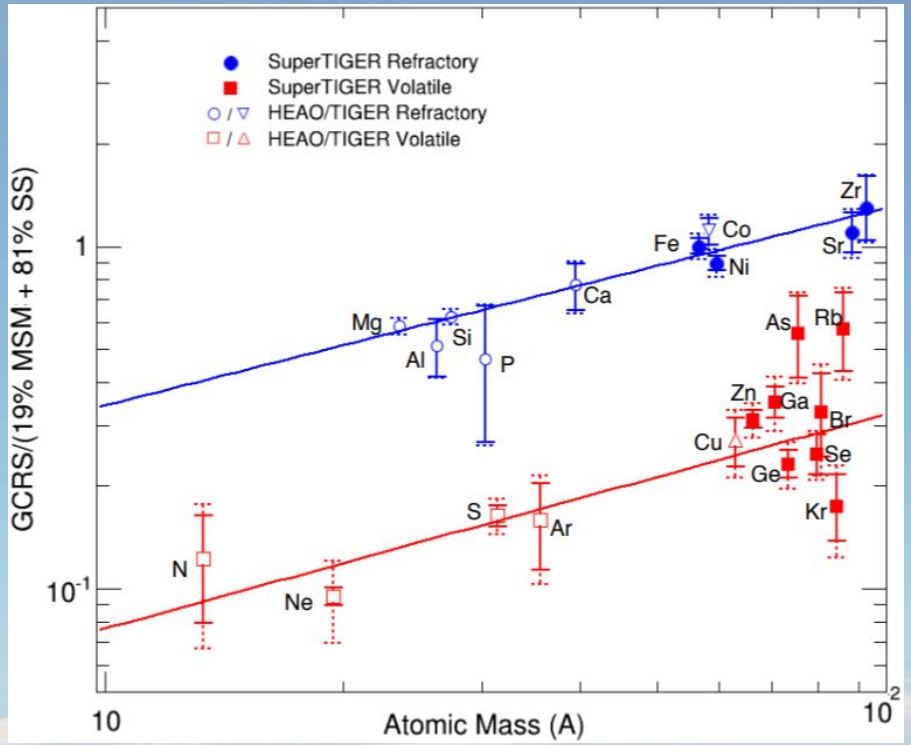

Murphy et al. 2016

- Plotting the GCRS abundances relative to a mixture of massive star material (MSM) with solar system reveals a clear refractory enhancement up to $_{40}$Zr
- This mixture is representative of OB associations, where the older interstellar medium (ISM) is enriched by newer MSM synthesized in and accelerated by frequent SNe
- Extending the GCRS measurement past $_{40}$Zr further tests this

The SuperTIGER Instrument

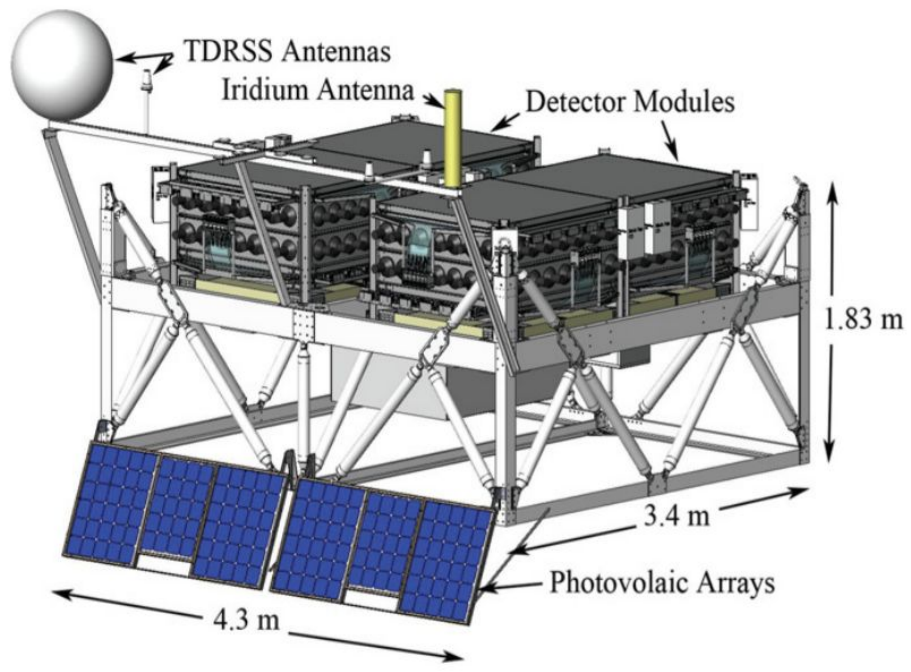

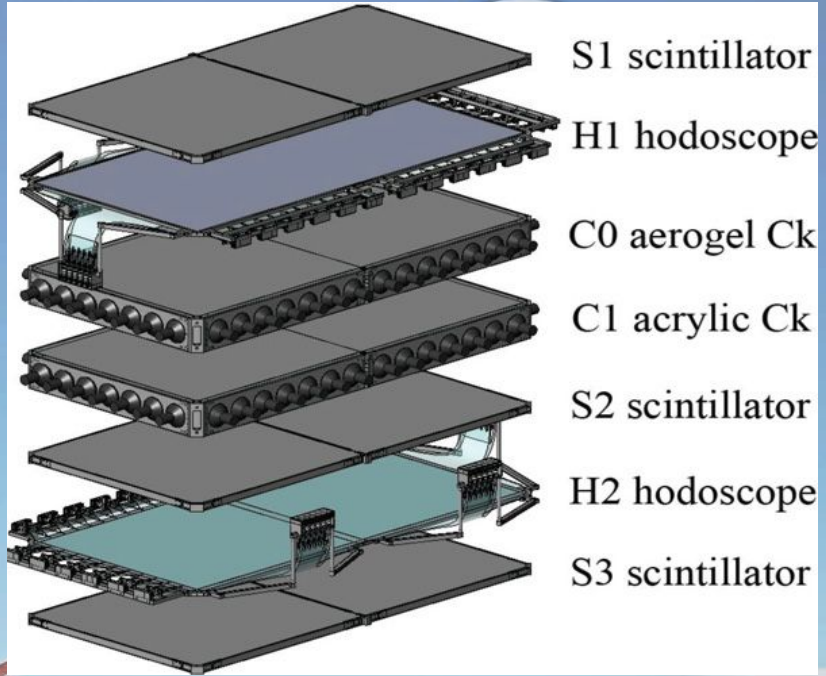

- Two, nearly identical, independent modules (shown mounted left, expanded view right)
- Each contains two scintillating fiber hodoscope planes (for particle trajectory), three scintillation detectors (for charge), and two Cherenkov detectors (for charge and energy)

Charge Assignment Method
- Signal Crossplot Charge Bands

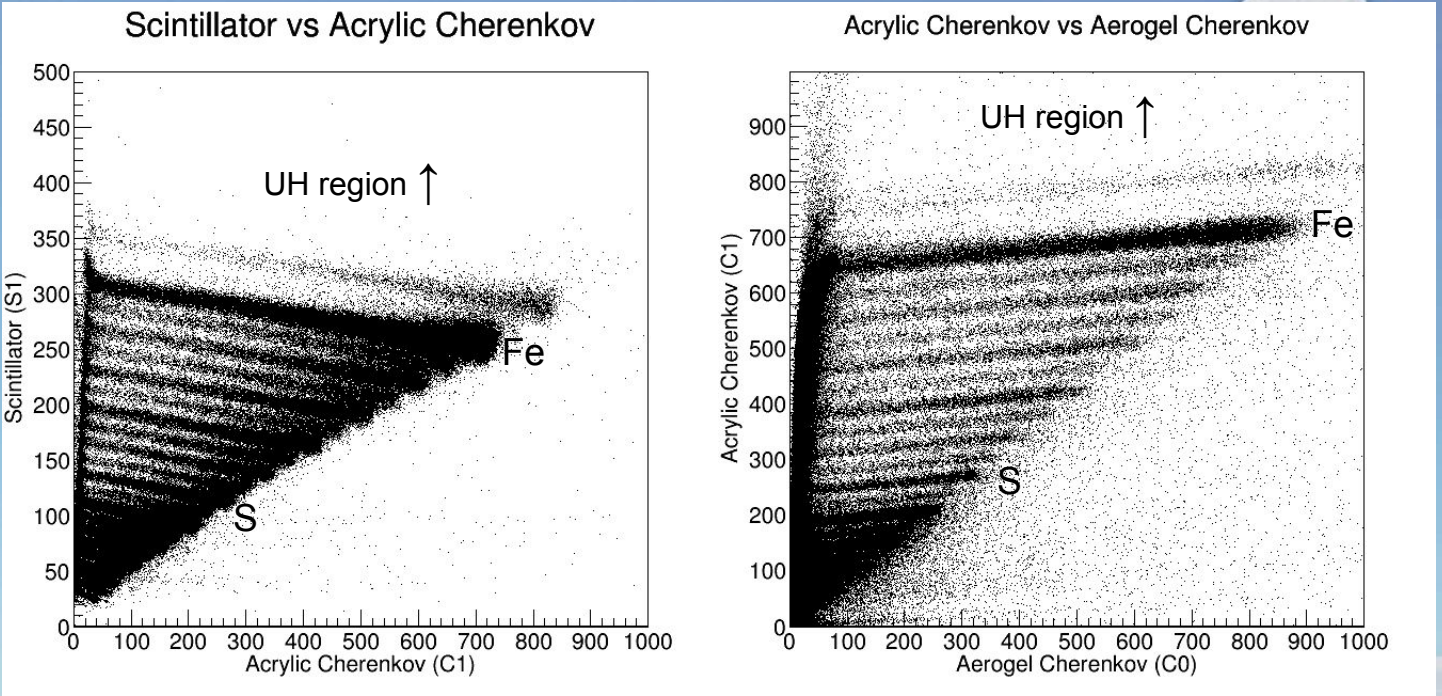

- Crossplots of the corrected signals (Makoto Sasaki, GSFC) from the scintillation and Cherenkov detectors reveal formation of charge bands
- Want to be able to assign charge where charge bands are not visible

Charge Assignment Method
- Above- and Below-C0 Methods

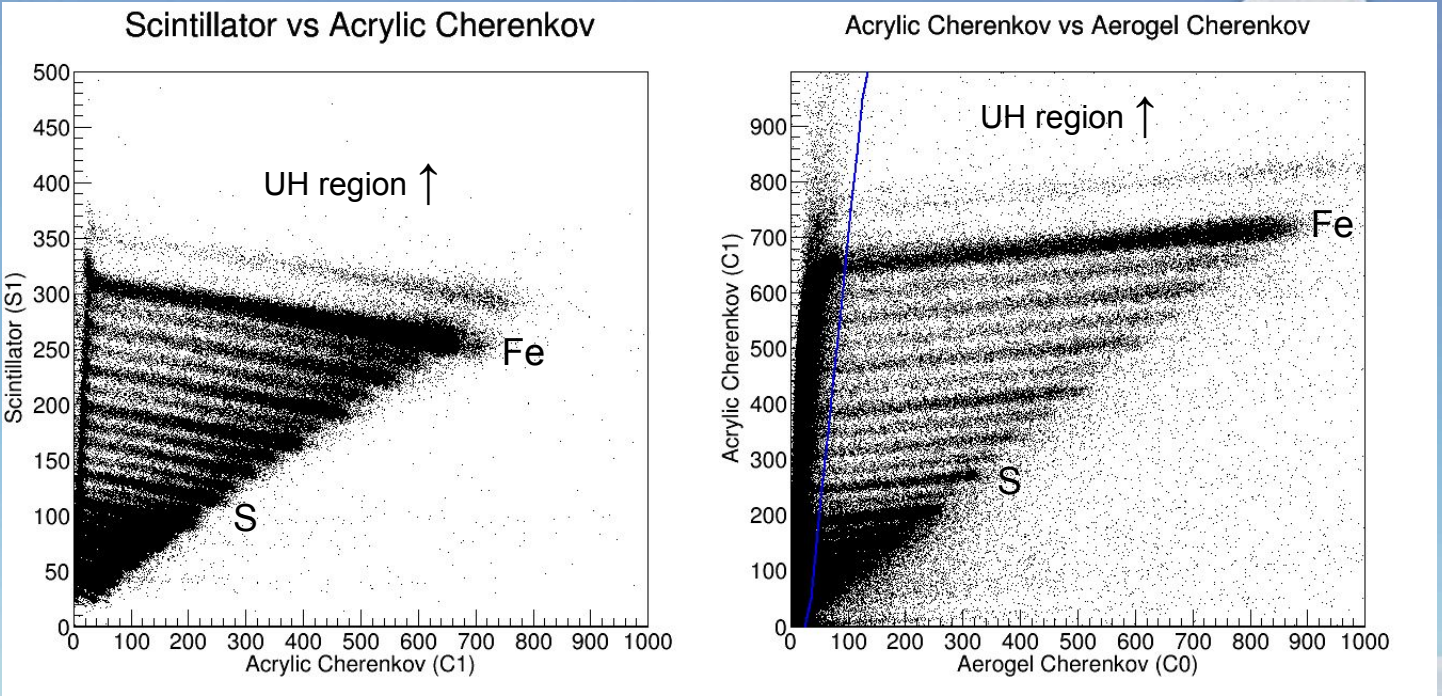

- A cut on the C1vsC0 crossplot separates the Above- and Below-C0 datasets
- Region to left of line (Aerogel threshold) is well resolved in the Below-C0 dataset
- Allows charge determination over most of the GCR energy range

Charge Assignment Method
- Band Spacing Charge Dependence

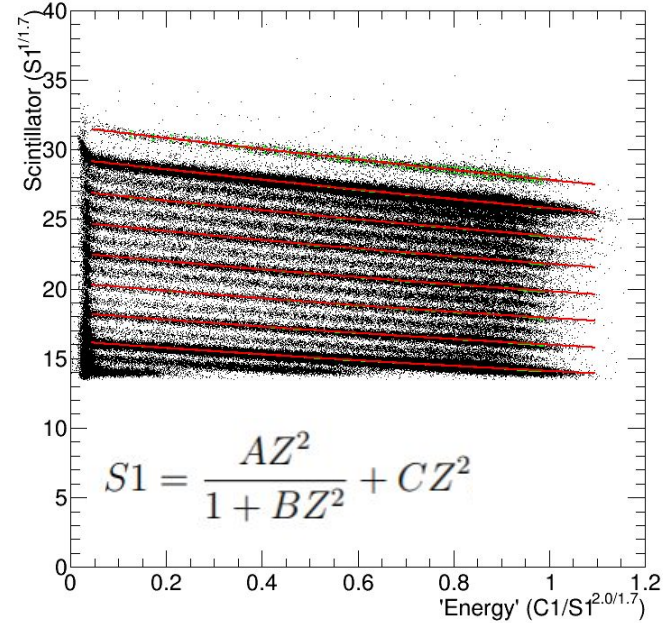

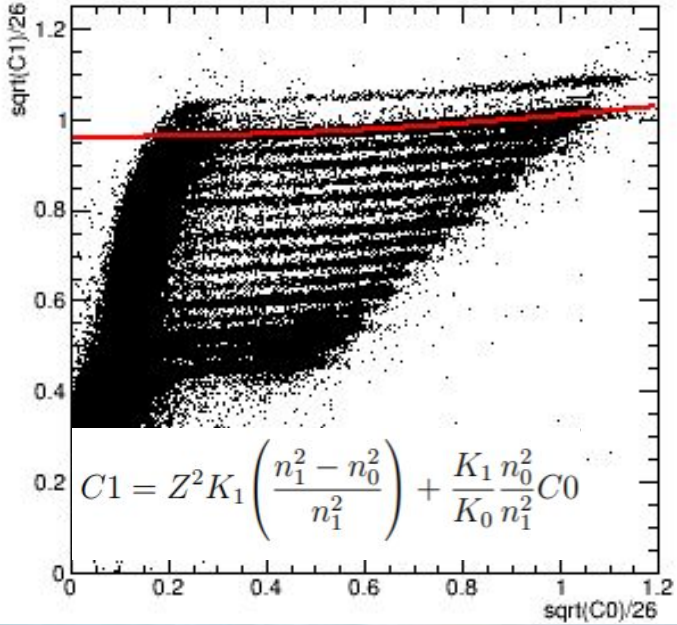

- Charge band fitting determines *Z* dependence of detector signals for every angle bin
- Different methods for Above-C0 (right) and Below-C0 (left) are extrapolated to higher signal space where high-*Z* events appear, but charge bands are not visible

Measured Abundances
- Charge Histogram

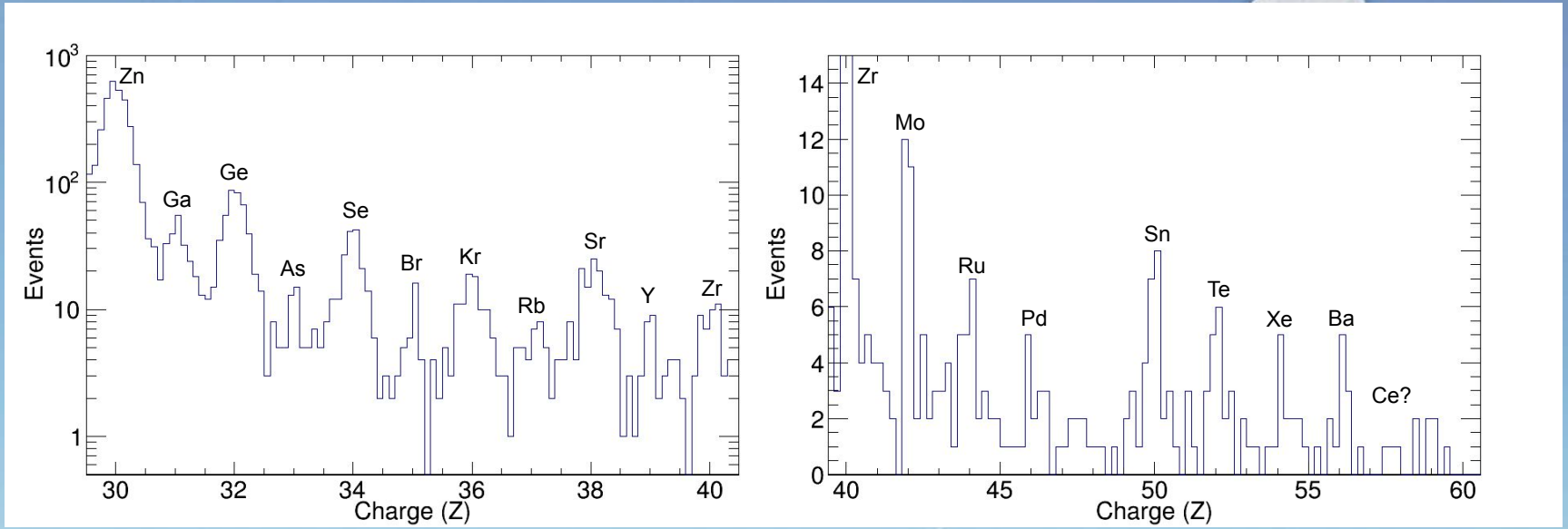

- *Z*>40 shows well defined peaks at even-*Z* elements but very low statistics and lack of clear element resolution at odd-*Z* elements
- *Z*=46&48 low relative to surrounding peaks (possible gain matching issue under investigation)

Measured Abundances
- Multipeak Gaussian Fitting

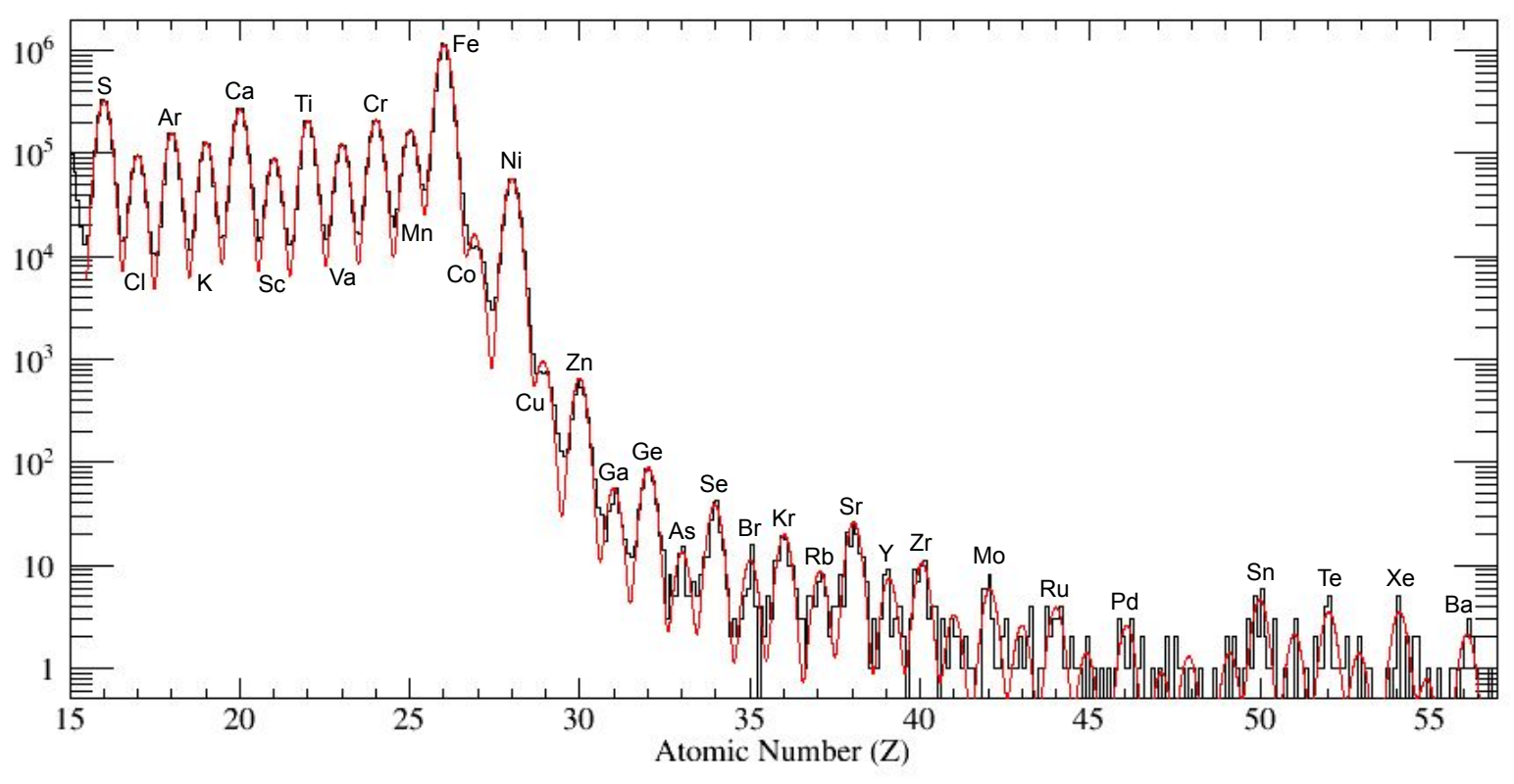

Comparison with Previous Observations - TOA Relative Abundances

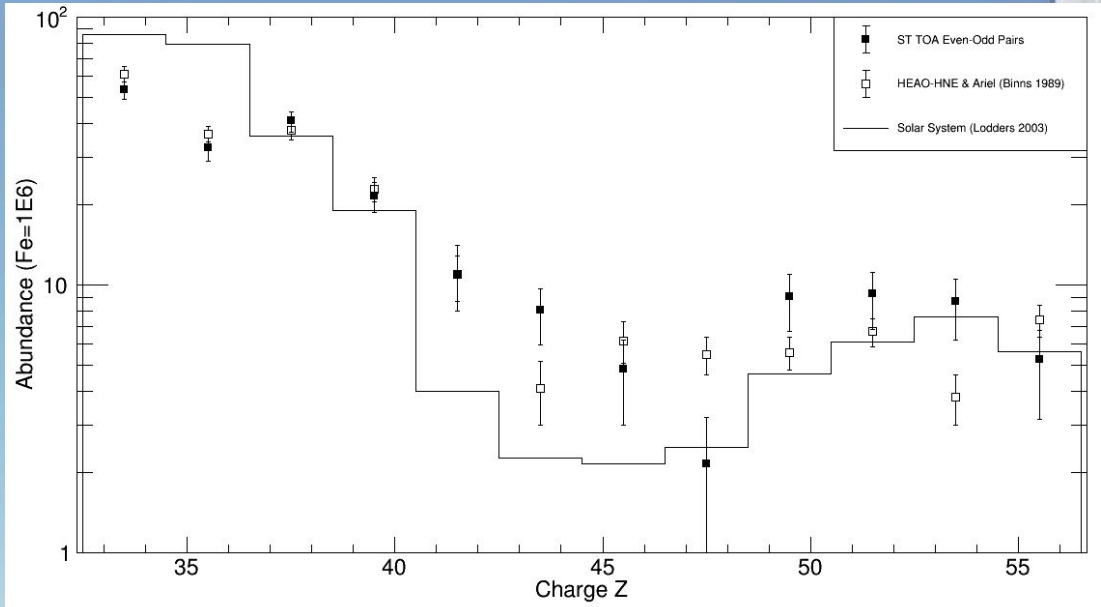

- Of particular interest is the consistency between the newly measured charge range and satellites HEAO-3 & Ariel that did not have individual element resolution and thus measured odd-even charge pairs

GCRS vs (80%SS + 20%MSM) - Model Breakdown for Z>40

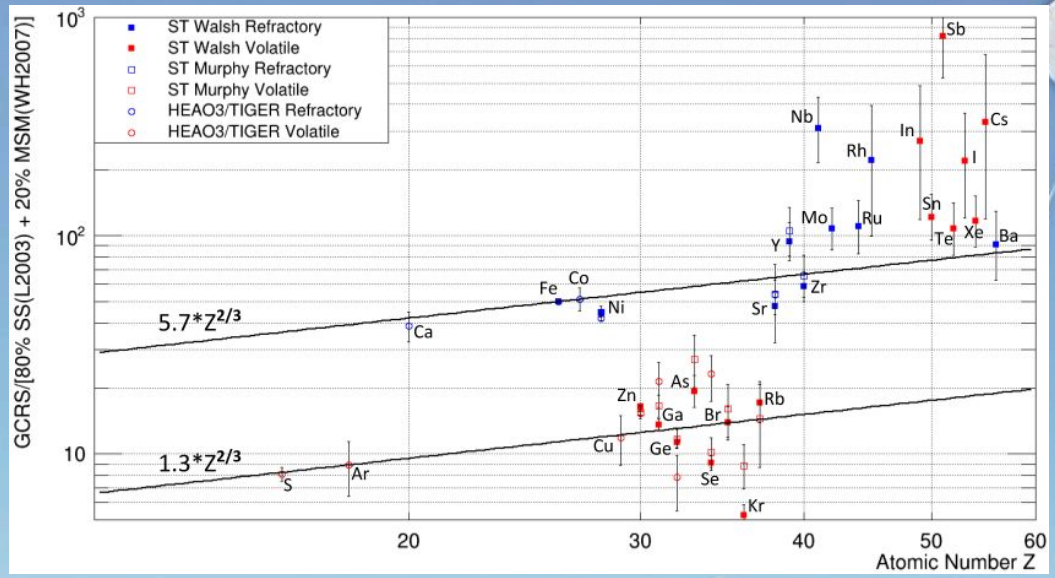

- The GCRS abundances suggest that the preferential acceleration of refractory elements by OB SNe seen for GCR with $Z \leq 40$ does not appear to hold for $Z > 40$
- Large statistical error bars on odd-$Z > 40$ elements due to very low statistics
- Will be elevated by uncorrected secondary contributions from even elements

GCRS vs (80%SS + 20%MSM) - Model Breakdown for Z>40

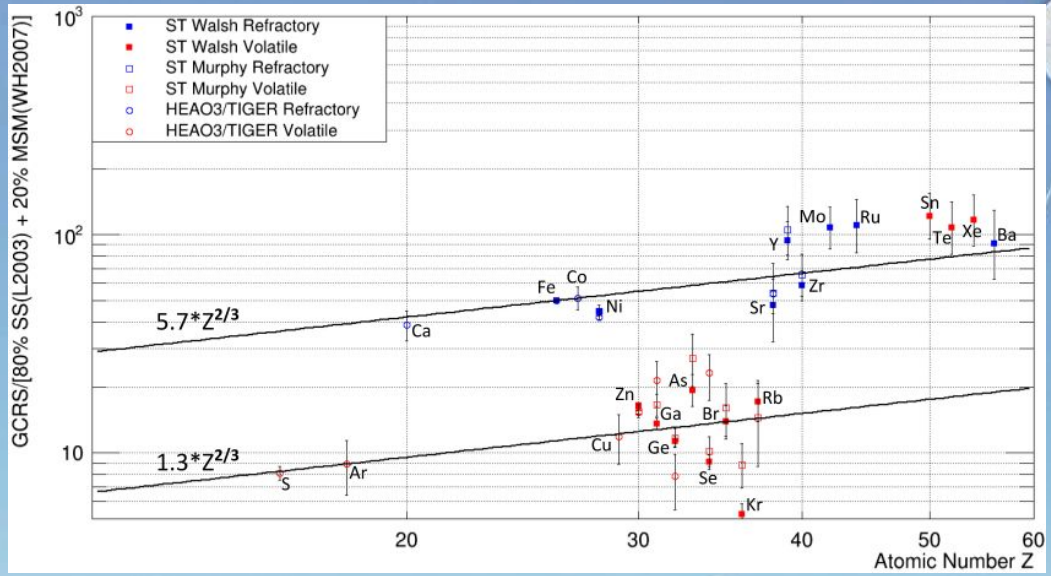

- The GCRS abundances suggest that the preferential acceleration of refractory elements by OB SNe seen for GCR with $Z \leq 40$ does not appear to hold for $Z > 40$
- Showing only even-$Z > 40$ elements, it appears that the volatiles are bumped up to the refractory line

Possible r-Process Enhancement?

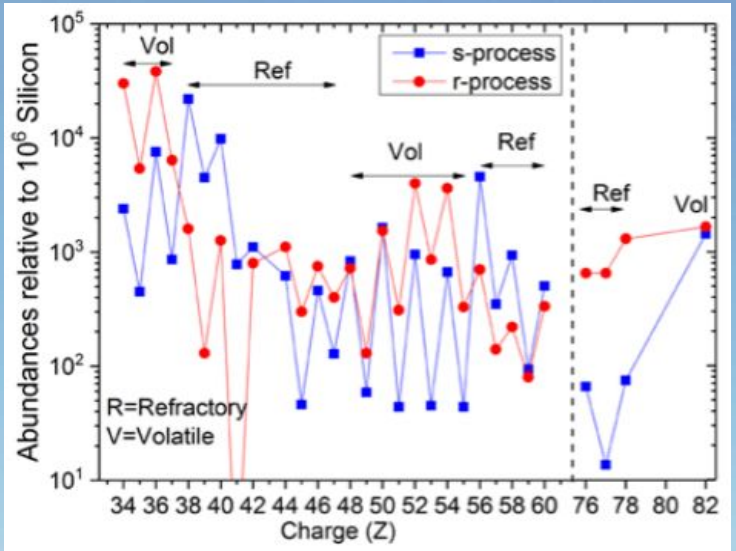

Binns (private communication)

- Breakdown of volatility based preferential SN shock acceleration model suggests that there is either a different production site or acceleration mechanism for $Z>40$
- All volatile elements with $Z>40$ have a large r-process component
- ACE-CRIS isotope measurements show a deficit of r-process GCR in the $30 \leq Z \leq 40$ range, but perhaps there is an excess of r-process GCR for $Z>40$

BNSM r-Process Production

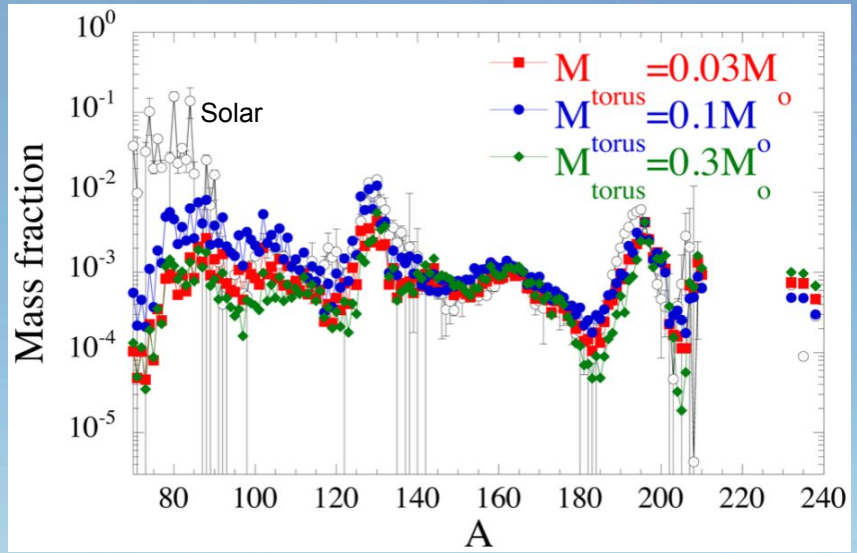

Just et al. 2015

- Binary neutron star mergers (BNSM), are known to produce vast amounts of r-process nuclei in a single event (LIGO/Virgo 2017 BNSM gravitational wave detection)
- Some BNSM models suggest that these events alone can account for the solar r-process abundances
- For $Z<40$ ($A<\sim90$) BNSM r-process production falls off
- It is interesting that this BNSM fall-off occurs at $Z=\sim40$, which is the point where the GCR source model appears to change

Thank You!

This research was supported by NASA under grants NNX09AC17G and NNX14AB25G, by the McDonnell Center for the Space Sciences at Washington University, and by the Peggy and Steve Fossett Foundation.

We thank the NASA Columbia Scientific Balloon Facility, the NASA Balloon Program Office, and the NSF United States Antarctic Program for the excellent and highly professional efforts that resulted in the record long-duration balloon flight for SuperTIGER and the successful recovery Effort.

Any opinions, findings, and conclusions or recommendations expressed in this material are those of the author(s) and do not necessarily reflect the views of the National Aeronautics and Space Administration.

John Mitchell | 7/13 @ 12:00 | The TIGERISS Experiment

Brian Rauch | 7/16 @ 18:00 | The Trans-Iron Galactic Element Recorder for the International Space Station (TIGERISS)

Brian Rauch | 7/16 @ 18:00 | Determination of Expected TIGERISS Observations

Backup Slides

Corrections for Interactions in the Instrument, Atmosphere and ISM

Top-of-Instrument

- Assume S1,S2 consistency cuts removed all charge-changing interactions

$$N_{TOI}(Z) = N_{INS}(Z) \prod_i \exp\left[\frac{x_i \langle \sec\theta_{Fe} \rangle}{\lambda_i(Z)}\right]$$

- Losses accounted for by adding these interacted events back in
- Instrument material thickness x_i are weighted averages of material seen by Above- and Below-C0 events

Top-of-Atmosphere

- Atmospheric interaction correction performed by Brian Rauch (Wash U)
- Iterative process that starts with an assumed set of TOA abundances and adjusts them until they yield the measured TOI abundances
- Losses given by total charge-changing cross sections
- Gains given by partial charge-changing cross sections

GCR Source

- ISM interaction and energy loss correction performed by Mark Wiedenbeck (JPL)
- Leaky-box based calculation accounts for losses and gains due to total and partial charge-changing interactions, radioactive decay paths and energy losses